60 61 62

63

64 65

66 67

68

69 70

76

77

78

79

80

81

82

83

84

85

86

87

88

89

90

91

92

93

94

95

96

97

98

99

100

101

102

103

104

105

106

107

108

109

110

111

112

113

114

115

116

117

118 119 120

121

ELSEVIER

Review Article

Operando methods: A new era of electrochemistry

Yao Yang^{1,2,3,4}, Julian Feijóo^{1,3}, Valentín Briega-Martos⁵, Qihao Li⁴, Mihail Krumov⁴, Stefan Merkens⁶, Giuseppe De Salvo⁶, Andrey Chuvilin^{6,7}, Jianbo Jin¹, Haowei Huang¹, Christopher J. Pollock⁸, Miquel B. Salmeron^{9,10}, Cheng Wang¹¹, David A. Muller^{12,13}, Héctor D. Abruña^{4,13} and Peidong Yang^{1,3,8,9,14}

Abstract

13

14

15

16

17

18

19

25

26

27

30

31

32

33

37

38

40

41

45

51

One of the grand challenges facing electrochemistry is to directly resolve the complex nature of (electro)catalyst active sites and capture real-time "movies" of reaction dynamics, i.e. "watching chemistry in action". The need for such fundamental understanding has stimulated the development of operando/in situ methods, which have greatly enhanced our ability to identify activity descriptors of electrocatalysts and establish structure-property relationships of energy materials. This review summarizes the frontiers of operando electrochemical liquid-cell scanning transmission electron microscopy and correlative synchrotron X-ray methods, which are complementary tools to comprehensively investigate reaction dynamics across multiple spatiotemporal scales. In an effort to encourage greater adoption of advanced operando methods by the general electrochemistry community, this review points out the need to benchmark electrochemistry in confined and heterogenous liquid environment with minimal beam-induced damage. We anticipate that multimodal operando methods will become indispensable for understanding interfacial reaction mechanisms for the broad chemistry and energy materials communities.

Addresses

- ¹ Department of Chemistry, University of California, Berkeley, CA, 94720, USA
- ² Miller Institute for Basic Research in Science, University of California, Berkeley, CA, 94720, USA
- ³ Chemical Sciences Division, Lawrence Berkeley National Laboratory, Berkeley, CA, 94720, USA
- Department of Chemistry and Chemical Biology, Cornell University, Ithaca, NY, 14853, USA
- ⁵ Forschungszentrum Jülich GmbH, Helmholtz-Institute Erlangen-Nürnberg for Renewable Energy (IEK-11), Cauerstr. 1, 91058, Erlangen, Germany
- ⁶ Electron Microscopy Laboratory, CIC NanoGUNE BRTA, Tolosa Hiribidea 76, Donostia, San Sebastián, 20018, Spain
- Ikerbasque, Basque Foundation for Science, Bilbao, 48013, Spain
 Cornell High Energy Synchrotron Source, Cornell University, Ithaca, NY, 14853, USA
- ⁹ Materials Sciences Division, Lawrence Berkeley National Laboratory, Berkeley, CA, 94720, USA
- ¹⁰ Department of Materials Science and Engineering, University of California, Berkeley, CA, 94720, USA

- ¹¹ Advanced Light Source, Lawrence Berkeley National Laboratory, Berkeley, CA, 94720, USA
- School of Applied and Engineering Physics, Cornell University, Ithaca, NY, 14853, USA
- ¹³ Kavli Institute at Cornell for Nanoscale Science, Cornell University, Ithaca, NY, 14853, USA
- ¹⁴ Kavli Energy NanoScience Institute, Berkeley, CA, 94720, USA

Corresponding author: Yang, Yao (yaoyang1@berkeley.edu)

Current Opinion in Electrochemistry xxxx, xxx:xxx

This review comes from a themed issue on Innovative Methods in Electrochemistry (2023)

Edited by Emmanuel Maisonhaute and Jay D.Wadhawan

For a complete overview see the Issue and the Editorial

Available online xxx

https://doi.org/10.1016/j.coelec.2023.101403

2451-9103/© 2023 Published by Elsevier B.V.

Keywords

Operando methods, Electrochemical interfaces, Electrocatalysis, Energy materials, Scanning transmission electron microscopy, Synchrotron X-rays.

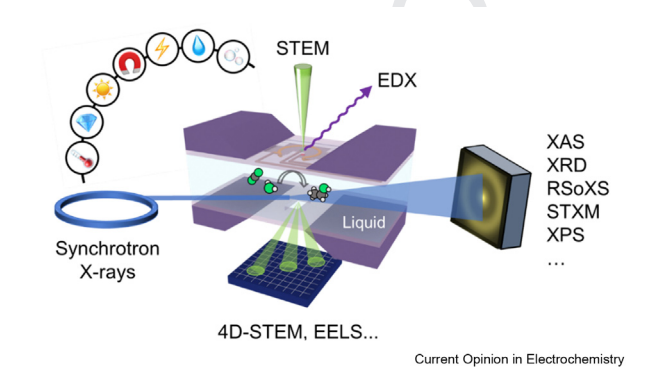
Electrochemistry lies at the interfaces among chemistry, physics and materials science and represents one of the more promising approaches for enhancing energy efficiency, mitigating environmental impacts and carbon emissions, and enabling renewable energy technologies, such as fuel cells, CO_2 and N_2 reduction, water splitting and post lithium-ion secondary batteries [1,2]. The past decades have witnessed the tremendous development in analytical instruments in the context of measurement science [3]. Recent advances in scanning transmission electron microscopy (STEM) and synchrotron X-ray methods have revived the field of electroanalytical chemistry [4]. Here, we review the latest breakthroughs of operando/in situ methods with an emphasis on electrons and X-rays as complementary structural probes of solid—liquid interfaces. For other analytical techniques,

60

interested readers are encouraged to read reviews on *operando/in situ* optical microscopy and spectroscopy (UV–Vis, IR and Raman), differential electrochemical mass spectrometry (DEMS), scanning electrochemical microscopy (SECM), scanning electrochemical cell microscopy (SECCM), nanoimpact electrochemistry and electrochemical quartz microbalance (EQCM) [1,4–8] (see Scheme 1).

First, we would like to give a clear definition of ex situ, in situ and operando. Ex situ methods provide a baseline understanding of pristine or postmortem samples. *In situ* methods simulate one or some of the reaction conditions but still deviate from realistic (device-level) operating conditions. Operando methods emphasize achieving multiple experimental conditions to fully sustain a working (electro)catalyst in an operating device [5,8]. Given the term in situ has been widely used in the past decades and operando is just emerging and requires considerable efforts to achieve device-level operation, this review provides flexibility regarding the precise boundary between in situ and operando methods and serves primarily as a roadmap to inspire readers to contribute to the advancement of operando methods. For electrochemistry, operando methods are defined here as analytical techniques that provide a comparable driving force (applied potential) to achieve a comparable reaction rate (current density), relative to standard electrochemical cells [4]. This review will first introduce recent breakthroughs in developing multimodal operando/in situ methods [9,11], particularly operando electrochemical liquid-cell STEM (EC-STEM) and correlative synchrotron X-ray methods. Selected examples of representative STEM or TEM (S/TEM), hard and soft X-ray methods will be discussed in detail. Particular attention is paid to beam-induced effects on

Schematic 1



Multimodal *operando* STEM and correlative X-ray methods: A powerful complementary toolbox. The upper left schematic includes a variety of stimuli (temperature, pressure, light, magnetic fields, electrical bias, liquid or gas environment) that may alter (electro)chemical reaction dynamics at solid—liquid interfaces (Copyright by the authors).

samples in liquid cells [12]. It remains necessary to convince the electrochemistry community that *operando* EC-STEM and X-ray methods can deliver comparable electrochemical results to bench-top electrochemical measurements.

64

65

66

67

68

69

70

71

72

73

74

75

76

77

78

79

80

81

82

83

84

85

86

87

88

89

90

91

92

93

94

95

96

97

98

99

100

101

102

103

104

105

106 107

108

109

110

111

112

113

114

115

116

117

118

119

120

121

122

123

124

125

126

Electrons and X-rays are complementary tools for electrochemical reaction probing dynamics solid-liquid interfaces across multiple spatiotemporal scales. The customized electrochemical liquid cell serves as a multimodal platform to combine those two powerful structural probes (Schematic 1). In general, electron probes provide nm-to-atomic scale information of individual nanoparticles (NPs) in a localized environment, while synchrotron based X-rays interrogate a large ensemble of NPs with statistical analysis. For both electrons and X-rays, beam-induced damage needs to be minimized in order to reliably probe electrochemical reactions without perturbing them. Conventional TEM uses a parallel electron beam while STEM focuses an electron beam into a sub-Ångström probe, which scans across the sample and is then analyzed by an electron detector [13,14]. Operando EC-STEM enables quantitative electrochemistry and simultaneous acquisition of quantitative STEM imaging, four-dimensional (4D) diffraction imaging, electron energy loss spectroscopy (EELS) and energy dispersive X-ray (EDX) spectroscopy [9,15-17]. In comparision, synchrotron based Xrays are divided into hard X-rays (>5 keV), tender X-rays (1-5 keV) and soft X-rays (<1 keV). High-energy hard X-rays can penetrate mm or thicker samples in standard electrochemical cells or operating energy devices. Soft X-rays are more advantageous as a probe for surface and thin film electronic structures due to their large absorption cross-section and chemical sensitivity. Operando X-ray methods include X-ray absorption spectroscopy (XAS), X-ray diffraction (XRD), resonant soft X-ray scattering (RSoXS), scanning transmission X-ray microscopy (STXM), X-ray photoelectron spectroscopy (XPS), among others.

State-of-the-art operando/in situ S/TEM and X-ray studies are summarized in Table 1. Given the concise scope of this review, the table only includes reports that have demonstrated operando/in situ S/TEM or X-ray methods in liquid under electrochemical conditions. A comprehensive summary of early operando/in situ STEM and X-ray studies can be found in our early review [4]. Rows 2-5 cover the real- and reciprocal-space resolutions, temporal and energy resolutions of electron or Xray probes in the presence of liquid. Rows 6–7 include the output information of chemical compositions and crystal structures. The ideal multimodal operando methods are expected to resolve morphological and compositional changes in real space and structural changes in reciprocal space at high spatiotemporal resolutions without beam damage in liquid. The overview of Table 1 delivers the important message that no single

65 66

67

68

69

70

71

72

73

74

75

76

77

78

79

80

81

82

83

84

85

86

87

88

89

90

91

92

93

94

95

96

97

98

99

100

101

102

103

104

105

106

107

108

109

110

111

112

113

114

115

116

117

118

119

120

121

122

123

124

125

126

Yes

No

No

59

60

Table 1 Summary of state-of-the-art operando/in situ S/TEM and correlative X-ray methods in liquid under electrochemical conditions. Electrons and X-rays serve as complementary probes to study solid-liquid interfaces across multiple spatiotemporal scales. Operando Methods Real-Space Reciprocal-Space Chemical Crystal Structure Temporal Energy in Liquid under Resolution Resolution Resolution Resolution Composition Electro- chemical Conditions Second-level STEM imaging nm to atomic No N/A Quantitative No [9,15-24]scalescale imaging 4D-STEM diffraction nm to atomic sub-Å Seconds to N/A No Yes imaging [9,16,17] scale minutes STEM-EELS ~0.5 eV (without nm to atomic Minute-level Yes No [22,24,28,59] scale monochromator) ~0.1 eV (with monochromator) STEM-EDX [16.59] nm-scale No Minutes to hours ~100 eV Yes No TEM imaging nm-scale No Milliseconds to N/A No No

seconds

seconds

minutes

Seconds to

Minutes to hours

~1.5 eV

(Conventional)

0.5-0.75 eV

(HERFD)

N/A

Milliseconds to

sub-Å

No

No

[9,36-44]Hard XRD (CTR or sub-Å Milliseconds to N/A No No Yes XSWs) [46,47] seconds sub-Å Minutes to hours Hard X-rav 2 um N/A Yes Yes Microscopy (Coupled XRD or XRF) [48,50] Soft XAS (TFY or No No Minutes to hours ~0.1 eV Yes No TEY) [51-55] **RSoXS Coupled Soft** No sub-nm Milliseconds to ~0.1 eV Yes Yes XAS [56] seconds Soft STXM [10,57] 50 nm Nο Minutes to hours ~0.1 eV Yes No Coupled Soft XAS AP-XPS [58] No No Minutes to hours 0.1-0.5 eV Yes No technique can possibly satisfy such an ideal require-

ment. Therefore, multimodal techniques are highly desirable to provide comprehensive information and approach a complete understanding of complex solid—liquid interfaces [11]. Although aberrationcorrected STEM imaging can routinely achieve sub-A spatial resolution in vacuum, the imaging resolution of EC-STEM is often limited to a few nanometers by counting statistics, at a beam dose of 1-10 e⁻/Å² or lower to reliably study beam-sensitive samples in liquid [12,15–17]. Similarly, despite recently developed electron detectors achieving a kHz-level or higher imaging frame rate (i.e. ms-level or higher temporal resolution), most S/TEM studies in liquid are limited to second-level temporal resolution in order to achieve a sufficiently high signal-to-noise ratio (SNR) when imaging nanoscale features in liquid. In other words, the spatial and temporal resolutions are often determined by the maximum beam dose allowed in liquid samples rather than instrumental resolutions. Recently, the maximum useable imaging speed (MUIS) has been proposed as a new information metric to integrate the spatial and temporal resolutions of electron detectors [14]. The MUIS, as a function of the SNR, determines precision and accuracy of quantitative STEM measurements.

Nο

Yes

Yes

High-angle annular dark-field (HAADF) STEM imaging, based on elastic scattering of electrons, is quantitative since imaging intensity scales with atomic number (I $\propto Z^{1.7}$) [13]. Quantitative STEM imaging has been used to investigate dynamic metal electrodeposition [15], structural evolution of nanoscale electrocatalysts [9,16-19] and solid-electrolyte interphase formation of lithium batteries [20,21], among other energy applications [4,22]. HAADF-STEM imaging can maintain a high spatial resolution, particularly for high-Z nanoparticles in thick liquid, when compared to

[21.31-36.59.71]

Electron Diffraction

Hard XAS (XANES)

in conventional

[36-42], HERFD

[9,43,44] modes)

Hard XAS (EXAFS)

No

No

Selected Area

[35,59]

conventional bright-field (BF) TEM imaging [23,24]. The latest development in 4D-STEM significantly expands the capability of STEM from conventional imaging to enable structural analysis in liquid [25,26]. 4D-STEM, based on electron microscopy pixel array detector (EMPAD), can achieve single electron sensitivity, high dynamic range and fast readout speed (up to 10,000 frames/second) [14], which are crucial for low-dose electron diffraction of beam-sensitive samples in liquid. While 4D-STEM diffraction imaging in vacuum has been demonstrated to achieve sub-Å real-space resolution and sub-pm reciprocal-space resolution [27], 4D-STEM in liquid has revealed valuable structural information already with nm-scale real-space resolution and sub-A reciprocal-space resolution [9,16,17]. STEM based core-loss EELS signals (>50 eV) are compromised by multiple inelastic scattering in liquid and only resolvable when liquid layers are thinner than 200-300 nm below which mass transport for electrochemistry becomes challenging [23,24,28]. In comparison, valence EELS, below the optical gap of the electrolyte (about 1-6 eV), is effective to resolve features through liquid thickness up to 500-600 nm. Operando energy-filtered TEM imaging, based on valence EELS, was used to track rapid de-/lithiation dynamics of LiFePO₄ nanoparticles and corresponding concentration/depletion of the diffuse layer in liquid during battery cycles [24]. STEM-EDX analysis is particularly powerful for analyzing heavy elements due to the high penetration depth of X-rays through thick samples. Recent technical developments addressed the shadowing problem of the liquid-cell holder tip and enabled more X-rays to reach the EDX detector [29]. In addition, the equipment of dual or quadruple EDX detectors can achieve a high collection efficiency with a large solid angle of one Steradian or above, which can significantly lower the beam dose in order to achieve desirable nm-scale spatial resolution. When compared to the relatively slow scanning mode of STEM imaging, conventional bright field (BF) TEM imaging can serve as a complementary imaging mode to achieve a subsecond-level or higher temporal resolution with faster electron detectors. The spatial resolution of TEM imaging is limited by chromatic aberration due to multiple inelastic scattering in liquid [30], which can be mitigated through energy filtering or chromatic aberration correction [23]. Since the pioneering work by Ross et al. [31], TEM imaging has been widely used to probe interfacial electrochemical dynamics [32–36]. Selected area electron diffraction (SAED), despite the absence of spatial resolution, has been used to reveal valuable structural information on electroreduction of Cu₂O nanoparticles [35]. TEM imaging and SAED have the merit of being widely accessible to most institutions as long as a conventional TEM is available. In general, electron diffraction is more dose efficient than S/TEM imaging for retrieving structural information of crystalline materials in liquid [13,14]. This review anticipates

that the continuous development of STEM techniques in liquid, especially 4D-STEM diffraction imaging, will make significant contributions to the electrochemistry community.

64

65

66

67

68

69

70

71

72

73 74

75

76

77

78

79

80

81

82

83

84

85

86

87

88

89

90

91

92

93

94

95

96 97

98

99

100

101

102

103

104

105

106

107

108

109

110

111

112

113

114

115

116

117 118

119

120

121

122

123

124

125

126

Operando synchrotron X-ray methods have been developed over a long period of time and are instrumental in understanding electrochemical reactions at solid-liquid interfaces (Table 1). Hard XAS, including X-ray absorption near-edge structure (XANES) and extended Xray absorption fine structure (EXAFS), is the most widely used *operando* X-ray method for reliably probing electrochemical reactions due to the high penetration depth and minimal beam damage [36-44]. Hard XAS excites core electrons of bulk samples, e.g. 3d metal K edges, and can be used to probe the site symmetry and oxidation state of an absorbing atom as well as the distances and identities of its nearest neighbors. For example, XAS can probe electrochemically induced surface changes of NPs, which are sufficient to trigger spectroscopic differences in XANES for quantitative analysis of valence states due to the high surface-to-bulk ratio of NPs. EXAFS, on the other hand, is more useful for detecting surface undercoordination for nanoparticles smaller than about 20 nm (one monolayer (~3 A) of a 20 nm or larger spherical NP corresponds to less than 10% contribution from the surface) [9]. XANES of first—row transition metals, collected in transmission mode, has an edge energy resolution of ~1.5 eV using a conventional solid-state detector with an energy resolution of 50–200 eV. The recent development of detecting XAS using a high resolution crystal spectrometer has given rise to high-energy-resolution fluorescence detected (HERFD) XAS, which enables much higher energy resolution—on the order of 0.5-0.75 eV— and allows for unprecedented information to be extracted from pre-edges [9,43–45]. This improved resolution comes at the price of signal intensity: While high quality HERFD XANES can be collected quickly, HERFD EXAFS requires significantly more time in order to achieve good SNR at high k for high resolution data. Hard X-ray diffraction, in particular crystal truncation rod (CTR) and X-ray standing waves (XSWs), enable an atomic-scale understanding of the electrode-electrolyte interfaces by decoupling surface changes from the bulk substrate. Both CTR and XSWs require well-defined, ideally single-crystal metal or oxide electrode surfaces [46,47]. Hard X-ray microscopy and correlative XRD have been used to penetrate mmthick electrode samples and electrolytes and provided um-level spatial resolution for dynamic de-/lithiation processes in batteries and oxygen evolution electrocatalysts [48-50]. In comparison to hard X-rays, soft XAS offers the twin advantages of producing much higher resolution spectra (~ 0.1 eV) and directly, via dipole-allowed transitions, probing the d orbital manifold of an absorbing 3d metal, which is sensitive to changes of metals' chemical environment. The main

65

66

67

68

69

70

71

72

73

74

75

76

77

78

79

80

81

82

83

84

85

86

87

88

89

90

91

92

93

94

95

96

97

98

99

100

101

102

103

104

105

106

107

108

109

110

111

112

113

114

115

116

117

118

119

120

121

122

123

124

125

126

47

49

50

51

52

53

54

55

56

57

58

59

60

challenges facing soft X-ray studies are the beaminduced damage due to larger inelastic scattering cross section and the design of vacuum-compatible liquid cells [51–55]. Soft XAS can be collected in either bulksensitive (hundreds of nm) total fluorescence yield (TFY) or surface-sensitive (<10 nm) total electron yield (TEY). Electron-vield XANES (EY-XANES) has been developed to probe interfacial water structure under electrochemical conditions [51]. Recently, operando resonant soft X-ray scattering (RSoXS) was developed to combine soft XAS studies of chemical environment and X-ray scattering of interparticle dynamics using a similar liquid-cell holder as EC-STEM [56]. Soft scanning transmission X-ray microscopy (STXM) was developed to provide nm-scale spatial resolution with simultaneous acquisition of an XAS spectrum [10,57]. Given an intense soft X-ray beam is focused into a nanoprobe, soft STXM has a high demand for sample stability in liquid under long-time beam exposure. Finally, in situ ambient pressure X-ray photoelectron spectroscopy (AP-XPS) can partially simulate electrochemical reaction conditions (a few torr with a thin liquid film) and has been reported to investigate chemical bonding on electrode surfaces [58].

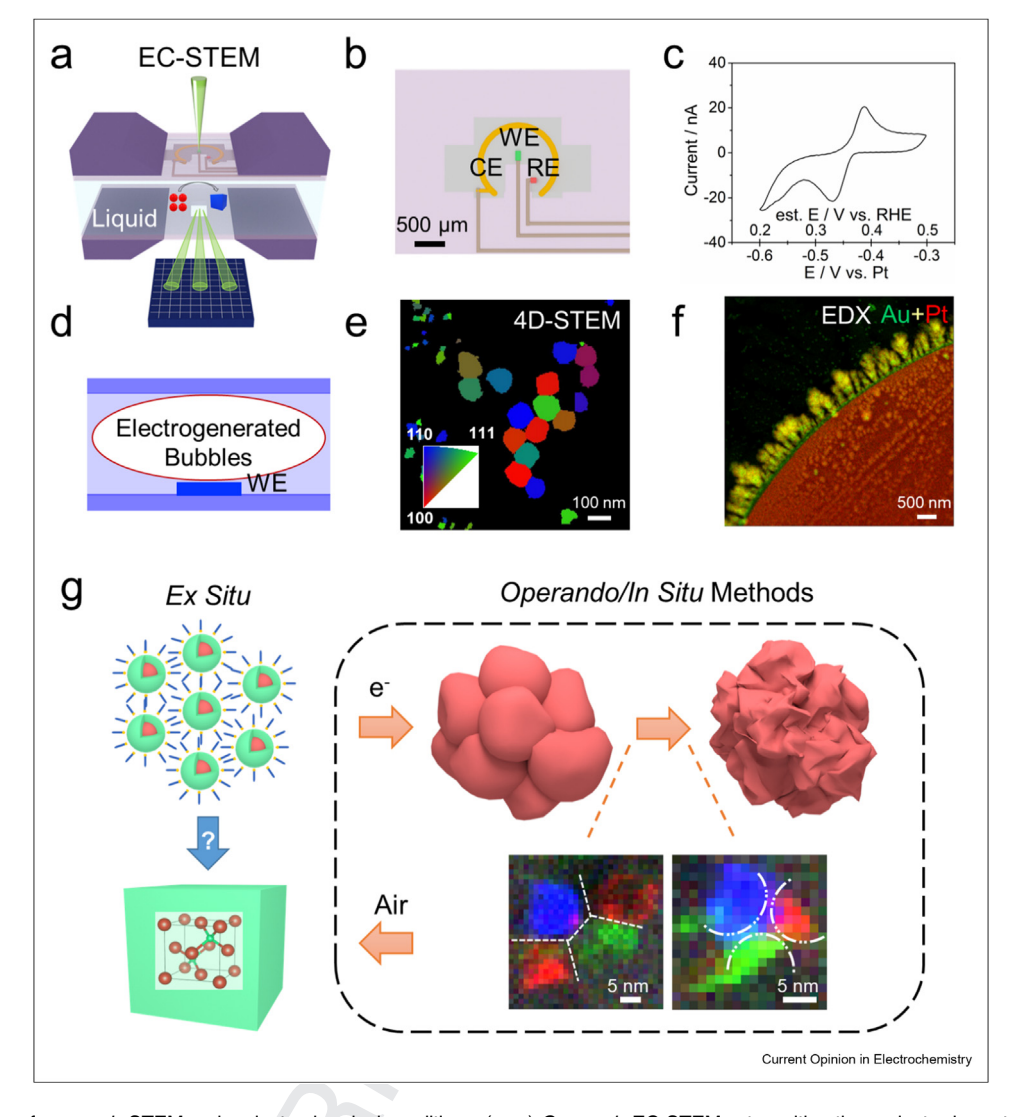
> Operando EC-STEM enables quantitative electrochemistry and simultaneous STEM imaging, 4D-STEM diffraction, EELS and EDX spectroscopy (Figure 1a) [9,15-17]. The central component of the EC-STEM is an electrochemical liquid cell with a three-electrode system of a carbon working electrode (WE), Pt counter and reference electrode (CE, RE, Figure 1b) [17]. A common EC-STEM holder often encapsulates electrolyte between two electron-transparent SiN_x windows with a spacer of 500 nm. Figure 1c presents a cyclic voltammetric (CV) profile of Cu NPs with welldefined redox couple of Cu₂O/Cu with the conversion from Pt pseudo-RE to reversible hydrogen electrode (RHE) estimated to be around 0.8 V [17]. The natural formation of electrogenerated H₂ bubbles under reducing potentials generates a thin-liquid layer (~100 nm) that remains electrochemically accessible (Figure 1d) [16,17]. This unique strategy enables operando EC-STEM to expand beyond conventional imaging of morphological changes and allows for 4D-STEM, EELS and EDX analysis (Figure 1e-f) [14]. The first demonstration of operando 4D-STEM in liquid was performed to reveal crystallographic orientation mapping of Au-Pt bimetallic alloys during cathodic corrosion (Figure 1e). The thin-liquid layer also enables the acquisition of STEM-EDX mapping of heterogeneous Au—Pt nanostructures in liquid (Figure 1f). Recently, operando EC-STEM, equipped with 4D-STEM, and correlative X-ray methods were employed to elucidate a longstanding challenge of identifying Cu active sites for CO₂ reduction reaction (CO₂RR) to multicarbon products [9]. This study provides, for the first time, the definitive evidence of metallic Cu nanograins, rich in

nanograin boundaries, supporting undercoordinated Cu active sites for C-C coupling (Figure 1g). Operando correlative methods provide a comprehensive life cycle of Cu nanocatalysts in which NP ensembles evolve into metallic Cu nanograins under CO₂RR before complete oxidation to single-crystal Cu₂O nanocubes upon air exposure [9]. Two false-color operando 4D-STEM diffraction imaging in liquid shows the complex structure of metallic Cu nanograin boundaries as possible active sites for CO2RR.

The customized electrochemical liquid-cell holder is compatible with not only operando EC-STEM but also resonant soft X-ray scattering (RSoXS, Figure 2a, c) [56]. Operando RSoXS provides a statistically robust analysis of dynamic aggregation processes of large ensembles of Cu NPs, complementing operando EC-STEM studies of individual Cu NPs. The major modification of the liquid-cell microchip for soft X-rays is the design of a dual carbon WE. Given the soft X-ray beam size is comparable to the electrode size, Cu NPs on window 1 are exposed to soft X-rays while those on window 2 experience the same electrochemical conditions but without X-ray exposure. Such a rigorous control experiment is essential to reliably investigate Cu@Cu₂O NPs that are subject to rapid soft X-ray beam-induced oxidation to CuO in the electrolyte [56]. Operando RSoXS enables simultaneous acquisition of soft XAS to study valence state during electroreduction of Cu₂O and X-ray scattering to study interparticle dynamics (Figure 2b, d). The NP-NP distance of 18 nm NP ensembles was measured to be 2.5 nm and decreased by 3 Å during CO₂RR. To accurately quantify valence state, HERFD was employed to enable hard X-rays with <1 eV-level energy resolution by exclusively selecting particular emission lines, such as Cu $K\alpha_1$ and thus suppressing the 1s core-hole lifetime broadening [4]. The pre-edge peaks are barely resolvable between Cu and Cu₂O in conventional XANES (Figure 2e). In comparison, the pre-edge peaks in HERFD XANES become markedly different (8979.9 eV for Cu; 8981.0 eV for Cu₂O, Figure 2f). The pre-edge peak of CuO at 8977.6 eV, due to Jahn-Teller distortion, is clearly shown in HERFD XANES but absent in conventional XANES. Quantitative analysis of *operando* HERFD XANES shows that all 7 nm NPs are converted to fully metallic Cu nanograins (Figure 2g-h) [9]. Such comprehensive multimodal operando methods represent a milestone in providing critical evidence of metallic Cu as active sites for CO₂RR. We anticipate that the continuous advances in operando X-ray methods, together with operando EC-STEM, will be instrumental in tackling the complex dynamic evolution of nanoscale electrocatalysts.

The level of impact of operando EC-STEM and X-ray methods on the electrochemistry community depends on how quantitatively we understand the electrochemical behaviors in liquid cells that are customized

Figure 1

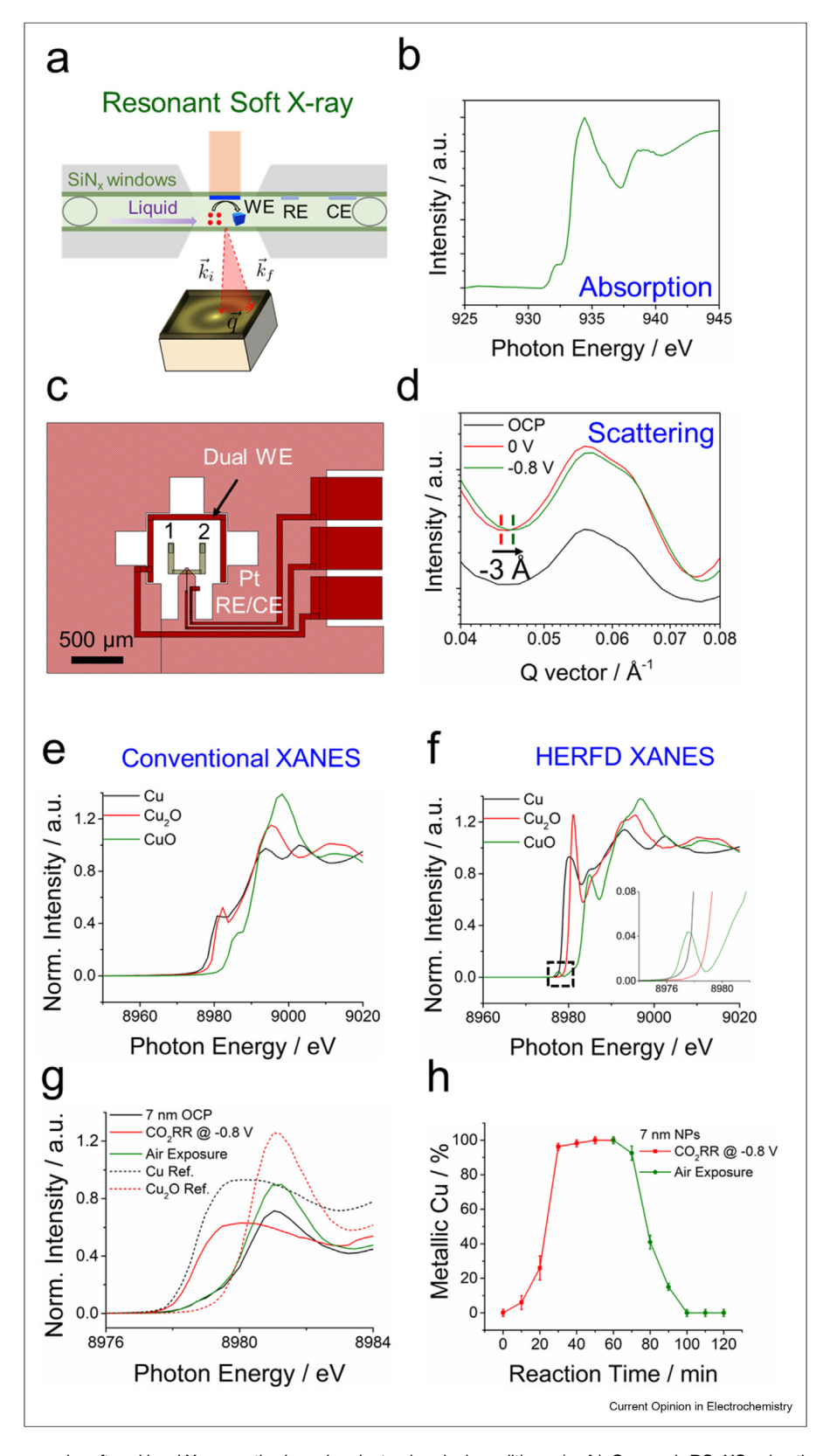


Selected examples of *operando* STEM under electrochemical conditions. (**a**-**c**) *Operando* EC-STEM setup with a three-electrode system and CV profiles of Cu NPs in CO₂-saturated 0.1 M KHCO₃ (adapted from a study by Yang et al. [17]. Copyright (2023) American Chemical Society). (**d**-**f**) Electrogenerated H₂ bubbles under reducing potentials create a native thin liquid layer (~100 nm), which enables 4D-STEM diffraction imaging (**e**) and STEM-EDX (**f**) of Au-Pt bimetallic alloys formed under electrochemical conditions (adapted from a study by Yang et al. [16]. Copyright (2022) American Chemical Society). (**g**) Compared to limited insights from *ex situ* methods, *operando/in situ* electrochemical 4D-STEM and correlative X-ray methods uncovered the dynamic evolution from Cu@Cu₂O nanoparticles to metallic Cu nanograins under bias and transformation to Cu₂O cubes upon air exposure (adapted from a study by Yang et al. [9]. Copyright (2023) Springer Nature).

for *operando* measurements [17,21]. In order to encourage the general electrochemistry community to adopt *operando* EC-STEM and X-ray methods, it is necessary to better understand how mass transport and kinetic equations of standard electrochemistry experiments change as a result of the unique geometry of *operando* cells, *i.e.* it is necessary to benchmark electrochemistry in confined and heterogenous liquid layers. Figure 3a presents the well-defined redox couple of Cu electrodeposition and stripping on Au nanocube electrode surfaces as a function of scan rate. A log—scale plot of the reduction peak current vs. scan rate shows a

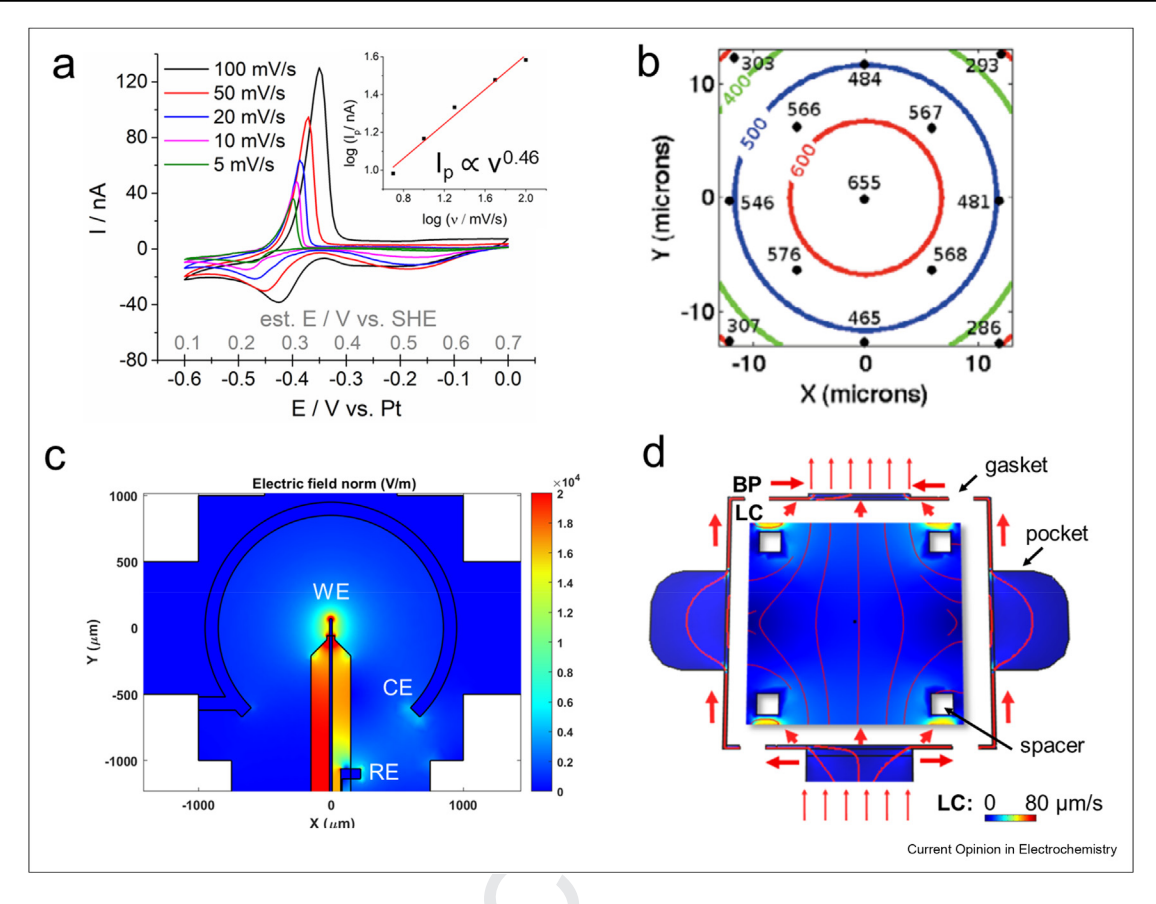
square-root relation, which is characteristic of a diffusion-controlled process [15]. Further analysis based on the Randles—Ševčík equation estimated the diffusion coefficient of Cu^{2+} to be 3.4×10^{-5} cm²/s. This is within the same order of magnitude when compared to the value reported in the literature $(7.4 \times 10^{-6} \text{ cm}^2/\text{s})$ for 1 mM Cu^{2+} in standard (bulk) cells, which suggests that the microelectrode in EC-STEM shows a bulk diffusion behavior, despite the confined sub- μ m thick liquid layer [15]. The window bulging, a result of pressure differences between the liquid cell and the TEM chamber, makes the liquid thicker in the middle

Figure 2



Selected examples of operando soft and hard X-ray methods under electrochemical conditions. (a-b) Operando RSoXS using the same liquid-cell holder as EC-STEM with a three-electrode system including a dual carbon WE. (c-d) Operando RSoXS enables the simultaneous acquisition of soft XAS and X-ray scattering (Figures a-d were adapted from a study by Yang et al. [56]. Copyright (2022) American Chemical Society). (e) Working principle of HERFD XAS (f-g) Comparison of XANES spectra of Cu, Cu₂O and CuO in conventional and HERFD modes. Inset in (f) showing the presence of a unique pre-peak of CuO only detectable in HERFD mode (Figures e-h were adapted from a study by Yang et al. [9]. Copyright (2023) Springer Nature).

Figure 3



Benchmark electrochemistry in confined and heterogenous liquid environment. (a) CV profiles of Cu electrodeposition and stripping in 1 mM CuSO₄/0.1 M NaClO₄ in EC-STEM holder (adapted from a study by Yang et al. [15]. Copyright (2022) American Chemical Society). (b) EELS measurements of liquid thickness variation for water with a 150 nm spacer in between two $25 \times 25 \,\mu\text{m}^2$ SiN_x windows (adapted from a study by Holtz et al. [20]. Copyright (2013) Microscopy Society of America). (c) Finite element simulation of the heterogeneous electric field distribution in vacuum of a three-electrode system with a WE potential of -1 V vs. RHE and CE potential of 2 V vs. RHE (Copyright by the authors). (d) Numerically simulated flow velocity profile of a liquid cell (LC) with realistic consideration of 2% off-chip bypass (BP) and a spacer of 150 nm. Red lines indicate direction and background color represents relative magnitude of flow velocity. The black square in the center reflects $20 \times 20 \,\mu\text{m}^2$ viewing window (adapted from a study by Merkens et al. [62]. Copyright (2023) Elsevier). (For interpretation of the references to color in this figure legend, the reader is referred to the Web version of this article.)

of the window and, thus, more challenging to resolve nanoscale features (Figure 3b) [20]. Liquid thickness can be estimated using the plasmon peak in the EELS spectrum and applying Beer's Law. The strategy of electrogenerated H₂ bubbles works well for electrochemical applications under reducing potentials [16,17], but there is a need to advance nanofabrication for a pristine liquid layer of 100 nm or thinner without forming gas bubbles [59].

In confined liquid cells, the electric field distribution and liquid flow are spatially heterogeneous [4,21]. Figure 3c shows the electric field map of the three-electrode system in vacuum using finite element simulations assuming a typical CO₂RR condition with a WE potential of -1 V vs. RHE (reversible hydrogen electrode). The significantly higher electric field around the tip of the WE has a profound tip-enhanced effect on the

evolution dynamics of nanoparticles. Recent liquid-cell TEM studies show pronounced aggregation of nanoscale features at the edge or tip of the WE while particle evolution in the central part of the WE shows a more homogenous and better potential-dependent control [9,34]. Thus, we emphasize the need to report the relative imaging location in the electrochemical chip and make close comparisons between evolution dynamics in liquid-cell STEM and that in standard electrochemical cells. Liquid flow is typically applied for continuous supply of fresh electrolyte and/or removal of species created in electrochemical (or radiolytic) processes in the liquid cell, but also allows to change the composition through solution replacement and in situ mixing [30,59,61]. Solute diffusion is an inherent mass transport mechanism induced by concentration gradients arising either due to external supply of solutes or their local generation during (electro-)chemical reactions.

65

66

67

68

69

70

71

72

73

74

75

76

77

78

79

80

81

83

84

85

86

87

88

89

90

91

92

93

94

95

96

97

98

99

100

101

102

103

104

105

106

107

108

109

110

111

112

113

114

115

116

117

118

119

120

121

122

123

124

125

126

Q3

32

33

35

36

37

38

39

40

41

42

43

44

45

46

47

49

50

51

52

53

54

55

56

57

58

59

60

Figure 3d presents the hydrodynamic quantification of a realistic liquid-cell flow setup based on its experimentally validated 3D flow channel geometry and reveals significant heterogeneity in mass transport rates across the nanochannel [62]. The relative velocity is noticeably higher on the side of the microchip than the middle region with realistic consideration of liquid bypassing along the chip edge. Continuous development of new liquid-cell geometries will provide EC-STEM setups with a well-defined mass transport and microfluidic dynamics [63].

In conclusion, this review summarizes recent advances in developing operando STEM based imaging, 4D-STEM diffraction, EELS and EDX spectroscopy, and correlative synchrotron hard and soft X-ray based absorption, diffraction, scattering and microscopy in liquid under electrochemical conditions. Multimodal operando EC-STEM and X-ray methods have been demonstrated to serve as complementary probes to elucidate the complex nature of active sites and dynamic evolution at unprecedented spatiotemporal resolutions. We emphasize the importance of demonstrating faithful electrochemical results in liquid cells without interference of beam-induced damage and the need for close comparisons to standard electrochemical measurements. We lay out several key points for operando EC-STEM and correlative X-ray methods to be widely accessible with simple and reliable operation for the broad chemistry and energy materials community:

- (1) The spatial resolution of STEM in liquid is often limited to a few nanometers by maximum beam dose applied to samples rather than instrument resolutions. The low beam dose (a few e⁻/Å²) in EC-STEM often requires a beam current of a few pA or lower [9,15-17,24]. Thus, EC-STEM has the potential to be widely applicable with a more affordable non-aberration-corrected STEM and a normally bright electron gun instead of an expensive aberration-corrected STEM with a very bright electron gun. Additional benefits of non-aberrationcorrected STEM are a larger depth of focus [64], particularly useful for thick liquid samples, and easier alignment and maintenance for general use.
- (2) Quantification of electrochemistry by developing standard reference electrodes with mV-level potential stability to replace Pt pseudo RE [65].
- (3) Correlations of multimodal *operando* methods across fields: Correlation of individual STEM and/or X-ray techniques, correlation of electrons and X-rays as structural probes with molecular probes (vibrational spectroscopy) [1,5,8], online product detection (DEMS) [9,66,67], online inductively coupled plasma (ICP) MS [68] and local activity (SECM) [10,69,70]. This combined approach will contribute to elucidating complex structural evolution under realistic electrochemical conditions, which

- otherwise will be impossible to comprehend with individual techniques [11,71].
- (4) Synchronization of electrochemical measurements with EC-STEM or X-ray data acquisition with the development of integrated and automated data processing software.
- (5) Rapid processing and feedback of large 4D-STEM and X-ray datasets as the demand for spatial and temporal resolutions continues to increase the data size, which has the potential to incorporate the latest developments in machine learning [72].

Uncited references

[60].

Declaration of competing interest

The authors declare that they have no known competing financial interests or personal relationships that could have appeared to influence the work reported in this paper.

Data availability

Data will be made available on request.

Acknowledgments

This work was supported by Director, Office of Science, Office of Basic O2 Energy Sciences, Chemical Sciences, Geosciences, & Biosciences Division, of the U.S. Department of Energy under Contract DE-AC02-05CH11231, FWP CH030201 (Catalysis Research Program). Work at Cornell University (especially operando EC-STEM) was supported by the Center for Alkaline-Based Energy Solutions (CABES), an Energy Frontier Research Center (EFRC) program supported by the U.S. Department of Energy, under grant DE-SC0019445. This work made use of TEM facilities at the CCMR which are supported through the National Science Foundation Materials Research Science and Engineering Center (NSF MRSEC) program (DMR-1719875). This work also used TEM facilities at the Molecular Foundry was supported by the Office of Science, Office of Basic Energy Sciences, of the U.S. Department of Energy under Contract No. DE-AC02-05CH11231. This research used resources of the Advanced Light Source, which is a DOE office of Science User Facility under contract no. DE-AC02- 05CH11231. This work is based on research conducted at the Center for High-Energy X-ray Sciences (CHEXS), which is supported by the National Science Foundation (BIO, ENG and MPS Directorates) under award DMR-1829070.

References

Papers of particular interest, published within the period of review, have been highlighted as:

- of special interest
- ** of outstanding interest
- Yang Y, et al.: Electrocatalysis in alkaline media and alkaline membrane-based energy technologies. Chem Rev 2022, 122: 6117-6321, https://doi.org/10.1021/acs.chemrev.1c00331.
- Ross MB, Luna PD, Li Y, Dinh C-T, Kim D, Yang P, Sargent EH: Designing materials for electrochemical carbon dioxide recycling. Nat Catal 2019, 2:648-658, https://doi.org/10.1038/
- Abruña HD: Electrochemical interface: modern techniques for in situ interface characterization. New York: VCH: 1991.
- Yang Y, Xiong Y, Zeng R, Lu X, Krumov M, Huang X, Xu W, Wang H, DiSalvo FJ, Brock JD, Muller DA, Abruña HD: Operando

Current Opinion in Electrochemistry xxxx, xxx:xxx

www.sciencedirect.com

16

17

18

26

34

35

44

45

63

- methods in electrocatalysis. ACS Catal 2021, 11:1136-1178, https://doi.org/10.1021/acscatal.0c04789
- Bentley CL, Kang M, Unwin PR: Nanoscale surface structure—activity in electrochemistry and electrocatalysis. J Am Chem Soc 2019, 141:2179—2193. https://pubs.acs.org/doi/ 10.1021/jacs.8b09828.
- Stevenson KJ, Tschulik KA: Materials driven approach for understanding single entity nano impact electrochemistry. Curr Opin Electrochem 2017, 6:38-45, https://doi.org/10.1016/ i.coelec.2017.07.009.
- Bañares MA: Operando methodology: combination of in situ spectroscopy and simultaneous activity measurements under catalytic reaction conditions. Catal Today 2005, 100: 71-77, https://doi.org/10.1016/j.cattod.2004.12.017
- Weckhuysen BM: Snapshots of a working catalyst: possibilities and limitations of in situ spectroscopy in the field of heterogeneous catalysis. Chem Commun 2002:97-110, https:// doi.org/10.1039/B107686H.
- Yang Y, Louisia S, Yu S, Jin J, Roh I, Chen C, Fonseca Guzman MV, Feijóo J, Chen P, Wang H, Pollock CJ, Huang X, Shao Y-T, Wang C, Muller DA, Abruña HD, Yang P: *Operando* studies reveal active Cu nanograins for CO₂ electroreduction. Nature 2023, 614:262-269, https://doi.org/10.1038/s41586-022-05540-0.

This work employs *operando* EC-STEM, 4D-STEM and correlative hard and soft X-ray methods and provides, for the first time, definitive evidence on metallic Cu nanograins as active sites for CO2

- Mefford JT, Akbashev AR, Kang M, Bentley CL, Gent WE, Deng HD, Alsem DH, Yu Y-S, Salmon NJ, Shapiro DA, Unwin PR, Cheuh WC: Correlative *operando* microscopy of oxygen evolution electrocatalysts. *Nature* 2021, **593**:67–73, https:// doi.org/10.1038/s41586-021-03454-x.
- 11. van der Stam W: The necessity for multiscale in situ characterization of tailored electrocatalyst nanoparticle stability. Chem Mater 2023, 35:386-394, https://doi.org/10.1021/ acs.chemmater.2c03286.
- 12. de Jonge N, Houben L, Dunin-Borkowski RE, Ross FM: Resolution and aberration correction in liquid cell transmission electron microscopy. *Nat Rev Mater* 2019, 4:61–78, https:// doi.org/10.1038/s41578-018-0071-2.
- 13. Muller DA: Structure and bonding at the atomic scale by scanning transmission electron microscopy. Nat Mater 2009, 8:263-270, https://doi.org/10.1038/nmat2380.
- Philipp HT, Tate MW, Shanks KS, Mele L, Peemen M, Dona P, Hartong R, van Veen R, Shao YT, Chen Z, Thom-Levy J, Muller DA, Gruner SM: Very-high dynamic range, 10,000 frames/second pixel array detector for electron microscopy. Micro. Microanal 2022, 28:425–440, https://doi.org/10.1017/ S1431927622000174.
- Yang Y, Shao Y-T, Lu X, DiSalvo FJ, Abruña HD, Muller DA: Metal monolayers on command: underpotential deposition at nanocrystal surfaces: a quantitative operando electrochemical transmission electron microscopy study. ACS Energy Lett 2022, 7:1292–1297, https://doi.org/10.1021/ acsenergylett.2c00209.
- 16. Yang Y, Shao Y-T, Lu X, Yang Y, Ko HY, DiStasio RA,

 ** DiSalvo FJ, Muller DA, Abruña HD: Elucidating cathodic corrosion mechanisms with operando electrochemical transmission electron microscopy. *J Am Chem Soc* 2022, **144**: 15698–15708, https://doi.org/10.1021/jacs.2c05989.

This work demonstrates the first 4D-STEM in liquid.

- Yang Y, Shao Y-T, Jin J, Feijóo J, Roh I, Louisia S, Yu S, Fonseca Guzman MV, Chen C, Muller DA, Abruña HD, Yang P: Operando electrochemical liquid-cell scanning transmission electron microscopy (EC-STEM) studies of evolving Cu nanocatalysts for CO₂ electroreduction. ACS Sustainable Chem Eng 2023, 11: 4119-4124, https://doi.org/10.1021/acssuschemeng.2c06542.
- Yoon A, Grosse P, Rettenmaier C, Herzog A, Chee SW, Roldan Cuenya B: **Dynamic transformation of cubic copper catalysts** during CO₂ electroreduction and its impact on catalytic selectivity. *Nat Commun* 2021, **12**:6736, https://doi.org/10.1038/ s41467-021-27500-4.

19. Beermann V, Holtz ME, Padgett E, de Araujo JF, Muller DA, Strasser P: Real-time imaging of activation and degradation of carbon supported octahedral Pt-Ni alloy fuel cell catalysts at the nanoscale using in situ electrochemical liquid cell STEM. Energy Envion Sci 2019, 12:2476-2485, https://doi.org/10.1039/ C9EE01185D.

64

65

66

67

68

69

70

71

72

73

74

75

76

77

78

79

80

81

83

84

85

86

87

88

89

90

91

92

93

94

95

96

97

98

99

100

101

102

103

104

105

106

107

108

109

111

112

113

114

115

116

117

118

119

120

121

122

123

124

125

126

- 20. Sacci RL, Black JM, Balke N, Dudney NJ, More KL, Unocic RR: Nanoscale imaging of fundamental Li battery chemistry: solid-electrolyte interphase formation and preferential growth of lithium metal nanoclusters. Nano Lett 2015, 15: 2011-2018, https://doi.org/10.1021/nl5048626
- Bhatia A, et al.: In Situ liquid electrochemical TEM investigation of LiMn_{1.5}Ni_{0.5}O₄ thin film cathode for micro-battery applications. Small Methods 2022, 6:2100891, https://doi.org/10.1002/smtd.202100891.
- Unocic RR, Sacci RL, Brown GM, Veith GM, Dudney NJ, More KM, Walden II FS, Gardiner DS, Damiano J, Nackashi DP: Quantitative electrochemical measurements using in situ EC-S/TEM devices. Microsc Microanal 2014, 20:452-461, https:// doi.org/10.1017/S1431927614000166.

This work is one of the earliest reports on a systematic study of effects of electrode geometry and microfluidic conditions on electrochemical measurements

- Holtz ME, Yu Y, Gao J, Abruña HD, Muller DA: In situ electron energy-loss spectroscopy in liquids. Microsc Microanal 2013, 19:1027-1035, https://doi.org/10.1017/S1431927613001505 This work remains a must-read on core-loss and valence-loss EELS in liquid.
- Holtz ME, Yu Y, Gunceler D, Gao J, Sundararaman R, Schwarz KA, Arias TA, Abruña HD, Muller DA: **Nanoscale im**aging of lithium ion distribution during in situ operation of battery electrode and electrolyte. Nano Lett 2014, 14: 1453-1459, https://doi.org/10.1021/nl404577c.
- Tate MW, Purohit P, Chamberlain D, Nguyen KX, Hovden R, Chang CS, Deb P, Turgut E, Heron JT, Schlom DG, Ralph D 25. Fuchs GD, Shanks KS, Philipp HT, Muller DA, Gruner SM: High dynamic range pixel array detector for scanning transmission electron microscopy. *Microsc Microanal* 2016, **22**: 237–249, https://doi.org/10.1017/S1431927615015664.
- Chen Z, Jiang Y, Shao YT, Holtz ME, Odstrcil M, Guizar-Sicairos M, Hanke I, Ganschow S, Schlom DG, Muller DA: Electron ptychorgraphy achieves atomic-resolution limits set by lattice vibrations. Science 2021, 372:826-831, https:// doi.org/10.1126/science.abg2533.
- 27. Padgett E, Holtz ME, Cueva P, Shao YT, Langenberg E, Schlom DG, Muller DA: The exit-wave power-cepstrum transform for scanning nanobeam electron diffraction: robust strain mapping at subnanometer resolution and subpicometer precision. *Ultramicroscopy* 2020, **214**:112994, https://doi.org/10.1016/j.ultramic.2020.112994.
- 28. Serra-Maia R, Kumar P, Meng AC, Foucher AC, Kang Y, Karki K, Jariwala D, Stach EA: Nanoscale chemical and structural analysis during in situ scanning/transmission electron microscopy in liquids. ACS Nano 2021, 15:10228-10240, https:// doi.org/10.1021/acsnano.1c02340.
- 29. Lewis E, Haigh SJ, Slater TJA, He Z, Kulzick MA, Burke MG, Zaluzec NJ: Real-time imaging and local elemental analysis of nanostructures in liquids. Chem Commun 2014, 50: 10019-10022, https://doi.org/10.1039/C4CC02743D.
- Klein KL, Anderson IM, de Jonge N: Transmission electron microscopy with a liquid flow cell. J Microsc 2011, 242: 117–123, https://doi.org/10.1063/1.4754271.
- 31. Williamson M, Tromp R, Vereecken P, Hull R, Ross FM: **Dynamic** microscopy of nanoscale cluster growth at the solid-liquid interface. Nat Mater 2003, 2:532-536, https://doi.org/10.1038/ nmat944

This study is the pioneering work demonstrating the feasibility of an electrochemical liquid-cell TEM using a two-electrode configuration.

Zeng Z, Zhang X, Bustillo K, Niu K, Gammer C, Xu J, Zheng H: In situ study of lithiation and delithiation of MoS₂ nanosheets using electrochemical liquid cell transmission electron microscopy. Nano Lett 2015, 15:5214-5220, https://doi.org/10.1021/acs.nanolett.5b02483.

65

66

67

68

69

70

71

72

73

74

75

76

77

78

79

80

81

83

84

85

86

87

88

89

90

91

92

93

94

95

96

97

98

99

100

101

102

103

104

105

106

107

108

109

110

112

113

114

115

116

117

118

119

120

121

122

123

124

125

126

- 8 9 10 11
- 12 13
- 14
- 15 16 17
- 18 19 20 21

22

23

24

25

26

27

28

29

30

31

32

33

35

36

37

38

39

40

41

42

43

44

45

46

47

49

50

51

52

53

54

55

56

57

58

59

60

61 62

63

- situ X-ray absorption spectroscopy of a synergistic Co-Mn oxide catalyst for the oxygen reduction reaction. *J Am Chem Soc* 2019, 141:1463–1466, https://doi.org/10.1021/jacs.8b12243.
- This study is the first operando XAS study of the synergistic effect of co-active sites in bimetallic oxides with a 3 mV potential resolution for tracking reaction dynamics.

acsnano.9b04745.

pnas.1918602117.

Xiong Y, Yang Y, Feng X, DiSalvo FJ, Abruña HD: A strategy for increasing the efficiency of the oxygen reduction reaction in Mn-doped cobalt ferrites. J Am Chem Soc 2019, 141: 4412-4421, https://doi.org/10.1021/jacs.8b13296.

33. Li Y, Kim D, Louisia S, Xie C, Kong Q, Yu S, Lin T, Aloni S,

Sci USA 2020, 117:9194-9201, https://doi.org/10.1073/

34. Wang X, Klingan K, Klingenhof M, Möller T, de Araújo JF,

Fakra S, Yang P: Electrochemically scrambled nanocrystals

are catalytically active for CO₂-tomulticarbons. Proc Natl Acad

Martens I, Bagger A, Jiang S, Rossmeisl J, Dau H, Strasser P:

Morphology and mechanism of highly selective Cu(II) oxide nanosheet catalysts for carbon dioxide electroreduction. Nat

copper nanocatalysts during the initial stages of the CO₂ reduction reaction. Angew Chem Int Ed 2021, 60:1347-1354,

Peña, et al.: Morphological and structural evolution of Co₃O₄

nanoparticles revealed by in situ electrochemical trans-

mission electron microscopy during electrocatalytic water

oxidation. ACS Nano 2019, 13:11372, https://doi.org/10.1021/

Yang Y, Wang Y, Xiong Y, Huang X, Shen L, Huang R, Wang H, Pastore JP, Yu S-H, Xiao L, Brock JD, Zhuang L, Abruña HD: *In*

Commun 2021, 12:794, https://doi.org/10.1038/s41467-021-

35. Vavra J, Shen TH, Stoian D, Tileli V, Buonsanti R: Real-time monitoring reveals dissolution/redeposition mechanism in

https://doi.org/10.1002/anie.202011137.

- Zeng R, Yang Y, Feng X, Li H, Gibbs LM, DiSalvo FJ, Abruña HD: Nonprecious transition metal nitrides as efficient oxygen reduction electrocatalysts for alkaline fuel cells. Sci Adv 2022, 8:eabj1584, https://doi.org/10.1126/sciadv.abj1584.
- Chang C-J, Lin S-C, Chen H-C, Wang J, Zheng KJ, Zhu Y, Chen HM: Dynamic reoxidation/reduction-driven atomic interdiffusion for highly selective CO₂ reduction toward methane. *J Am Chem Soc* 2020, 142:12119–12132, https:// doi.org/10.1021/jacs.0c01859.
- 41. Li J, et al.: Copper adparticle enabled selective electrosynthesis of n-propanol. Nat Commun 2018, 9:4614, https://doi.org/10.1038/s41467-018-07032-0.
- Kimura KW, Casebolt R, DaSilva JC, Kauffman E, Kim J, Dunbar TA, Pollock CJ, Suntivich J, Hanrath T: **Selective elec**trochemical CO₂ reduction during pulsed potential stems from dynamic interface. ACS Catal 2020, 10:8632-8639, https://doi.org/10.1021/acscatal.0c02630.
- 43. Friebel D, et al.: Identification of highly active Fe sites in (Ni,Fe)OOH for electrocatalytic water splitting. J Am Chem Soc 2015, 137:1305-1313, https://doi.org/10.1021/ja511559d.
- 44. Hung S-F, Chan Y-T, Chang C-C, Tsai M-K, Liao Y-F, Hiraoka N, Hsu C-S, Chen HM: Identification of stabilizing high-valent active sites by *operando* high-energy resolution fluorescence-detected X-ray absorption spectroscopy for high-efficiency water oxidation. *J Am Chem Soc* 2018, 140: 17263–17270, https://doi.org/10.1021/jacs.8b10722.
- 45. Hämäläinen K, Siddons DP, Hastings JB, Berman LE: Elimination of the inner-shell lifetime broadening in X-ray-absorption spectroscopy. *Phys Rev Lett* 1991, **67**:2850–2853, https://doi.org/10.1103/PhysRevLett.67.2850.
- Plaza M, Huang X, Ko JYP, Shen M, Simpson BH, Rodríguez-López J, Ritzert NL, Letchworth-Weaver K, Gunceler D, Schlom DG, Arias TA, Brock JD, Abruña HD: Structure of the photo-catalytically active surface of SrTiO₃. J Am Chem Soc 2016, 138:7816-7819, https://doi.org/10.1021/
- Abruña HD, Bommarito GM, Acevedo D: The study of solid/ liquid interfaces with X-ray standing waves. Science 1990, 250:69-74, https://doi.org/10.1126/science.250.4977.69.

- 48. Yu S-H, Huang X, Brock JD, Abruña HD: Regulating key variables and visualizing lithium dendrite growth: an operando Xray study. J Am Chem Soc 2019, 141:8441-8449, https:// doi.org/10.1021/jacs.8b13297
- Yu S-H, Huang X, Schwarz K, Huang R, Arias TA, Brock JD, Abruña HD: Direct visualization of sulfur cathodes: new insights into Li-S batteries via operando X-ray based methods. Energy Environ Sci 2018, 11:202-210, https://doi.org/10.1039/ c7ee02874a.
- 50. Kuai C, Xi C, Hu A, Zhang Y, Xu Z, Nordlund D, Sun C-J, Cadigan CA, Richards RM, Li L, Dong C-K, Du X-W, Lin F: Revealing the dynamics and roles of iron incorporation in nickel hydroxide water oxidation catalysts. J Am Chem Soc 2021, **143**:18519–18526, https://doi.org/10.1021/jacs.1c07975.
- 51. Velasco-Velez J-J, Wu CH, Pascal TA, Wan LF, Guo J, Prendergast D, Salmeron MB: The structure of interfacial water on gold electrodes studied by X-Ray absorption spectroscopy. Science 2014, 346:831-834. https://www.science.org/doi/ 10.1126/science.1259425
- 52. Ye Y, Wu CH, Zhang L, Liu Y-S, Glans-Suzuki P, Guo J: Using soft X-ray absorption spectroscopy to characterize electrode/ electrolyte interfaces in-situ and operando. J Electron Spectrosc Relat Phenom 2017, 221:2-9, https://doi.org/10.1016/ j.elspec.2017.05.002.
- Drake IJ, Liu TCN, Gilles M, Tyliszczak T, Kilcoyne ALD, Shuh DK, Mathies RA, Bell AT: **An** *in situ* cell for characterization of solids by soft X-ray absorption. Rev Sci Instrum 2004, 75:3242, https://doi.org/10.1063/1.1791320.
- Schwanke C, Xi L, Lange KM: A Soft XAS transmission cell for operando studies. *J Synchrotron Radiat* 2016, 23:1390, https:// doi.org/10.1107/S1600577516014697.
- Weatherup RS, Wu CH, Escudero C, Pérez-Dieste V Salmeron MB: Environment-dependent radiation damage in atmospheric pressure x-ray spectroscopy. J Phys Chem B 2018, 122:737-744, https://doi.org/10.1021/acs.jpcb.7b06397.
- Yang Y, Roh I, Louisia S, Yu S, Chen C, Jin J, Yu S, Salmeron MB, Wang C, Yang P: *Operando* resonant soft X-ray scattering studies of chemical environment and interparticle dynamics of cu nanocatalysts for CO₂ electroreduction. J Am Chem Soc 2022, 144:8927-8931, https://doi.org/10.1021 iacs.2c03662

This work is the first demonstration of electrochemical RSoXS and systematically investigates the soft X-ray beam-induced oxidation of Cu in liquid environments.

- Zhang C, Mille N, Eraky H, Stanescu S, Swaraj S, Belkhou R, Higgins D, Hitchcock A: Copper CO₂ reduction electrocatalysts studied by in situ soft X-ray spectro-ptychography. Chem-RXiv 2023, https://doi.org/10.26434/chemrxiv-2023-67dt2.
- Favaro M, Jeong B, Ross PN, Yano J, Hussain Z, Liu Z, Crumlin EJ: Unravelling the electrochemical double layer by direct probing of the solid/liquid interface. Nat Commun 2016, 7:12695, https://doi.org/10.1038/ncomms12695.
- 59. Beker AF, Sun H, Lemang M, van Omme JT, Spruit RG, Bremmer M, Basak S, Pérez-Garza HH: In situ electrochemistry inside a TEM with controlled mass transport. Nanoscale 2020, 12:22192-22201, https://doi.org/10.1039/D0NR04961A.
- Schneider NM, Norton MM, Mendel BJ, Grogan JM, Ross FM, Bau HH: Electron-water interactions and implications for liquid cell electron microscopy. J Phys Chem C 2014, 118: 22373-22382
- 61. Merkens S, De Salvo G, Chuvilin A: The effect of flow on radiolysis in liquid phase-TEM flow cells. Nano Express 2022, 3: 45006, https://doi.org/10.1088/2632-959X/acad18.
- 62. Merkens S, De Salvo G, Kruse J, Modin E, Tollan C, Grzelczak M, Chuvilin A: Quantification of reagent mixing in liquid flow cells for liquid phase-TEM. Ultramicroscopy 2023, 245:113654, https://doi.org/10.1016/j.ultramic.2022.113654

This study establishes realistic hydrodynamic models of microfluidic channels in confined liquid cells.

Merkens S, Tollan C, De Salvo G, Bejtka K, Fontana M, Chiodoni A, Grzelczak M, Seifert A, Chuvilin A: Towards sub-

17 18 19

- second solution exchange dynamics in liquid-phase TEM flow reactors. Research Square Preprint 2023, https://doi.org/ 10.21203/rs.3.rs-3208774/v1.
- 64. Xin HL, Muller DA: Aberration-corrected ADF-STEM depth sectioning and prospects for reliable 3D imaging in S/TEM. J Electron Microsc 2009, 58:157-165, https://doi.org/10.1093/
- Walker NL, Dick JE: Leakless bipolar reference electrode: fabrication performance and miniaturization. Anal Chem 2021, 93:10065-10074, https://doi.org/10.1021/ acs.analchem.1c00675.
- 66. Baltruschat H: Differential electrochemical mass spectrom**etry**. *J Am Soc Mass Spectrom* 2004, **15**:1693–1706, https://doi.org/10.1016/j.jasms.2004.09.011.
- 67. Wang H, Abruña HD: New insights into methanol and formic acid electro-oxidation on Pt: simultaneous DEMS and ATR-SEIRAS study under well-defined flow conditions and simulations of CO spectra. J Chem Phys 2022, 156, 034703, https://
- Fuchs T, Briega-Martos V, Drnec J, Stubb N, Martens I, Calle-Vallejo F, Harrington DA, Cherevko S, Magnussen OM: Anodic

and cathodic platinum dissolution processes involve different oxide species. Angew Chem Int Ed 2023, 62, e202304293, https://doi.org/10.1002/anie.202304293.

23

24

25

27

28

30

31

32

33

34

35

36

37

38

39

40

- 69. Mariano RG, McKelvey K, White HS, Kanan MW: Selective increase in CO₂ electroreduction activity at grain-boundary surface terminations. Science 2017, 358:1187-1192, https:// doi.org/10.1126/science.aao3691.
- Santos CS, Jaato BN, Sanjana I, Schuhmann W, Andronescu C: Operando scanning electrochemical probe microscopy during electrocatalysis. *Chem Rev* 2023, **123**:4972–5019, https://doi.org/10.1021/acs.chemrev.2c00766.
- Abdi, et al.: Understanding the dynamics of molecular water oxidation catalysts with liquid-phase transmission electron microscopy: the case of Vitamin B₁₂. ACS Sustainable Chem Eng 2021, 9:9494–9505, https://doi.org/10.1021/ acssuschemeng.1c03539.
- Shi C, Cao MC, Rehn SM, Bae S-H, Kim J, Jones MR, Muller DA, Han Y: Uncovering material deformations via machine learning combined with four-dimensional scanning transmission electron microscopy. npj Comput Mater 2022, 8:114, https://doi.org/10.1038/s41524-022-00793-9.